Fifth Symposium on Global Change Studies, January 23-28, 1994, Nashville, TN, pp. 262-269. American Meteorological Society.

TWO-CHANNEL MICROWAVE RADIOMETER FOR OBSERVATIONS OF TOTAL COLUMN PRECIPITABLE WATER VAPOR AND CLOUD LIQUID WATER PATH

J.C. Liljegren

Pacific Northwest Laboratory*
Richland, Washington, U.S.A.

1. INTRODUCTION

The Atmospheric Radiation Measurement (ARM) Program is focused on improving the treatment of radiation transfer in models of the atmospheric general circulation, as well as on improving parameterizations of cloud properties and formation processes in these models (USDOE, 1990). To help achieve these objectives, ARM is deploying several two-channel microwave radiometers at the Cloud and Radiation Testbed (CART) site in Oklahoma for the purpose of obtaining long time series observations of total precipitable water vapor (PWV) and cloud liquid water path (LWP), defined as

$$PWV = \frac{1}{\rho_L}\int_0^\infty \rho_V(z)\, dz \ , \quad (cm), \qquad (1)$$

$$LWP = \frac{1}{\rho_L}\int_0^\infty w(z)\, dz \ , \quad (mm), \qquad (2)$$

where ρ_L is the density of liquid water, $\rho_V(z)$ is the density of water vapor and w(z) is the cloud liquid water content (g m^{-3}).

Daily averages of PWV from 9 October 1992 through 21 July 1993 are presented in Figure 1. This data reveals the annual trend of low moisture content in the winter (PWV ≈ 0.5 cm) increasing to over 4 cm in the summer. Superimposed on the annual trend are the synoptic variations associated with frontal passages.

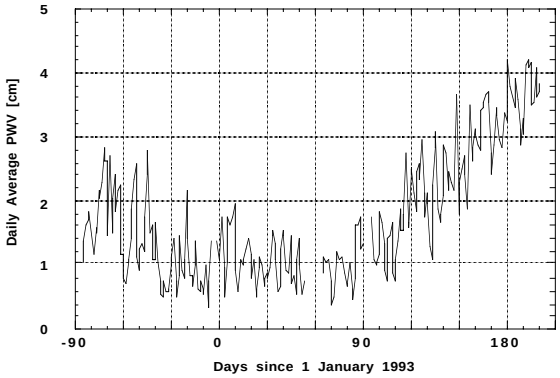

Figure 1. Daily averages of PWV from 9 October 1992 through 21 July 1993 at the ARM Cloud and Radiation Testbed (CART) central facility near Lamont, OK.

1.1 Background

Both PWV and LWP have been widely used to understand cloud and radiation interactions. For example, Stephens (1978) has shown that LWP is a useful surrogate for the cloud optical depth, $\delta = 3/2\ LWP/r_e$, where r_e is the effective droplet radius. This relationship has been exploited to parameterize cloud radiative properties and to study cloud structure; see for example Stephens (1984), Cahalan and Snider (1989), Cahalan and Wiscombe (1991). PWV is also used to parameterize atmospheric radiation transfer. For example Li *et al.* (1992) used PWV to relate net solar radiation at the surface to satellite-derived fluxes. Kuo *et al.* (1993) have shown that short-range precipitation forecasts and predictions of the vertical distribution of specific humidity are improved when PWV is assimilated into numerical weather prediction models.

The use of PWV and LWP for developing and testing radiation and cloud models imposes significant performance requirements for accuracy, sensitivity and long-term stability of the measurements. In this paper the performance of one of the ARM microwave radiometers with respect to these requirements is presented.

2. THE MICROWAVE RADIOMETER

The microwave radiometers (MWRs) that ARM has acquired are Radiometrics Model WVR-1100. These are dual-frequency instruments operating at 23.8 and 31.4 GHz. (See Table 1.) The 23.8 GHz channel is about three times as sensitive to water vapor as the 31.4 GHz channel; the 31.4 GHz channel is about twice as sensitive to liquid water as the 23.8 GHz channel. The two channels use a common antenna and waveguide system with individual Gunn diode oscillators for each

*Pacific Northwest Laboratory is operated for the U.S. Department of Energy by Battelle Memorial Institute under Contract DE-AC06-76RLO 1830.

Corresponding author address: James C. Liljegren, Pacific Northwest Laboratory, Battelle Blvd., Richland, WA 99352.

Table 1. WVR-1100 Specifications.

Vapor Sensing Channel	
Frequency	23.8 GHz
Bandwidth	0.4 GHz
Beamwidth (3dB)	5.5 degrees
Liquid Sensing Channel	
Frequency	31.4 GHz
Bandwidth	0.4 GHz
Beamwidth	4.6 degrees
Pointing Characteristics	
Angular coverage	4π sr
Angular slew rate	> 90 degrees/s, elevation 3 degrees/s, azimuth
Physical Characteristics	
Dimensions	58 x 28 x 74 cm
Weight	21 kg
Power	120 W max. (winter)
Voltage	90-135 VAC, 47-440 Hz

frequency. This design has two implications. First, simultaneous observations at the two frequencies are not possible - only one Gunn diode can be on at a time; and second, the fields of view of each channel are not identical. At 2 km altitude this translates into fields of view of 192 m (at 23.8 GHz) and 161 m (at 31.4 GHz). Considering the differences in the temporal and spatial scales of PWV and LWP, as well as the differences in the sensitivity of the channels to vapor and liquid, this difference in field of view is not particularly significant.

2.1 Radiometric Measurements

The MWR measures the incident microwave energy and reports it as an equivalent blackbody brightness temperature, T_{sky} (K) for each channel:

$$T_{sky} = T_{ref} + \frac{V_{sky} - V_{ref}}{G} . \quad (3)$$

T_{ref} (K) is the actual temperature of the ambient blackbody reference target, V_{sky} (counts) is the signal observed when viewing the sky, V_{ref} (counts) is the signal observed when viewing the reference target, and G is the system gain (counts K^{-1}). The gain is extremely sensitive to the temperature of the microwave hardware. The microwave hardware is mounted on an aluminum plate in an insulated enclosure and thermally stabilized to 323 ±0.2 K to ensure gain stability. Even so, to achieve the necessary accuracy the gain is measured during each observing cycle, defined below. This is accomplished by switching on a "hot load" in the form of a calibrated noise diode that injects microwave energy directly into the system. The gain is determined as

$$G = \frac{V_{ref+nd} - V_{ref}}{T_{nd}} . \quad (4)$$

V_{ref+nd} is the signal when viewing the reference target with the noise diode on, V_{ref} is the signal viewing the target with the noise diode off, and T_{nd} is the noise diode output (K) determined by prior calibration. (See below.) Combining Eqs (3) and (4) gives:

$$T_{sky} = T_{ref} + T_{nd} \frac{V_{sky} - V_{ref}}{V_{ref+nd} - V_{ref}} . \quad (5)$$

During each observing cycle, the three signals in Eq (5) are obtained for each channel. The mirror is rotated to view the sky; the Gunn diode oscillators for each channel are then sequentially energized and the signals recorded. The mirror is then rotated to view the blackbody target; for each channel the signals are recorded with the noise source off and on. The target temperature is measured and Eq (5) applied to determine the sky brightness temperature.

The above observing cycle acquires a 1-second "snapshot" of the sky every 20 seconds. This high sampling rate is necessary because the LWP measurements are being used to develop and test new models that describe the inhomogeneous nature of clouds. The sampling rate must be high in order to resolve the fine scale structure of clouds. Averaging over a longer period would tend to smear out the details. Sampling faster (by shortening the observing cycle, if possible) would not necessarily provide additional independent observations: for a 10 m s^{-1} wind speed at 2 km altitude, at least 16 seconds are required for a scene to advect through the field of view of the liquid sensitive channel.

2.2 Calibration

Absolute calibration is achieved by use of "tipping curves." (See Decker and Schroeder, 1991.) Essentially, the atmospheric optical depth at several elevation angles is measured using an old or estimated calibration, and a straight line is fitted against the cosecant of the elevation angle. The slope of the line is the true zenith optical depth, from which can be computed the true zenith brightness temperature. Tipping curves can only be performed on days when the sky is completely free of clouds as the technique assumes that the atmosphere is plane-parallel and horizontally homogeneous. In Oklahoma, such conditions have been rare during the last year.

Combined with measurements of the blackbody reference target, both with the noise diode switched off and on, the noise diode output can be calibrated as well. First, the gain is determined for each tipping curve by solving Eq (3)

$$G = \frac{V_{sky} - V_{ref}}{T_{sky} - T_{ref}} . \quad (6)$$

Equation (4) is then solved for T_{nd} and the gain computed from the tipping curve used to determine the noise diode output T_{nd}:

$$T_{nd} = \frac{V_{ref+nd} - V_{ref}}{G} . \quad (7)$$

The amount of microwave energy injected into the antenna system by the noise diode is not constant; rather ($V_{ref+nd} - V_{ref}$) is a random variable with a Gaussian distribution. To prevent adding noise into the calibration, tipping curves are performed at 90-second intervals over a period of hours and the mean value of T_{nd} for each channel is used. The distributions of T_{nd} resulting from the tipping curves are shown in Figure 2 for the 23.8 GHz (vapor-sensitive) channel and in Figure 3 for the 31.4 GHz (liquid-sensitive) channel.

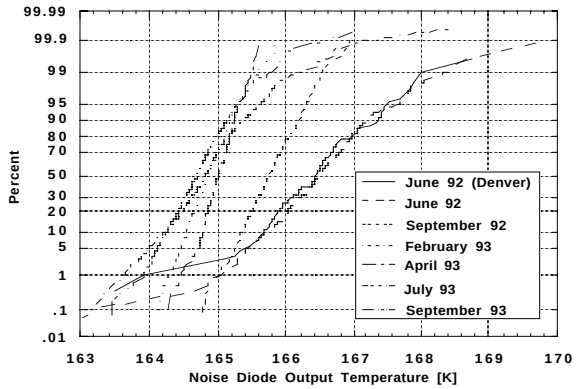

Figure 2. Noise diode output calibration history for the 23.8 GHz channel.

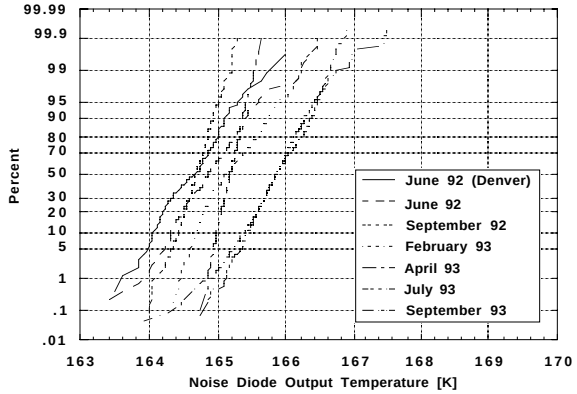

Figure 3. Noise diode output calibration history for the 31.4 GHz channel.

Calibration stability is important for long-term observations. Even though the tipping curves can be performed automatically by the MWR, collecting tipping curve data interrupts normal data collection. Fortunately, the interruptions occur during the least interesting periods, i.e. during clear sky conditions. The MWR calibrations exhibit a 1% overall variation over a period of more than a year. However, it is apparent that the aging of the noise diode is not linear in time. The mean value of T_{nd} for the 23.8 GHz channel appears to have reached a stable value; the mean value for the 31.4 GHz channel changed noticeably between the April and July calibrations, but remained constant from July to September.

3. CALCULATION OF PWV AND LWP

PWV and LWP are determined from the MWR brightness temperatures using a statistical retrieval technique developed by Westwater (1993).

3.1 Statistical Retrieval

Essentially, historical radiosonde data representing the climatology where the MWR will be operated are input to a model of microwave radiation transfer (Schroeder and Westwater, 1991). This model computes the zenith optical depths, δ, atmospheric mean radiating temperatures, T_{mr}, and the expected microwave brightness temperatures corresponding to each sounding:

$$T_{sky} = T_c\, e^{-\delta} + T_{mr}\,(1 - e^{-\delta}). \qquad (8)$$

T_c is the cosmic radiating temperature equal to 2.75 K.

For each sounding in the climatological data base the PWV is computed by integrating along the trajectory of the sounding and the LWP is computed by inserting clouds in regions of the sounding where the relative humidity exceeds a preset threshold value. The PWV and LWP are then related to the optical depths using multiple linear regressions of the form

$$PWV = a_0 + a_1\,\delta_{23.8} + a_2\,\delta_{31.4},$$

$$LWP = b_0 + b_1\,\delta_{23.8} + b_2\,\delta_{31.4}. \qquad (9)$$

The retrieval coefficients for Eq (9) have been computed for each calendar month by E.R. Westwater and M.J. Falls of NOAA/Wave Propagation Laboratory (WPL) using ten years of NWS radiosonde data from Oklahoma City, OK. Note that the observed brightness temperatures are related to the optical depths by solving Eq (8)

$$\delta = \ln\left(\frac{T_{mr} - T_c}{T_{mr} - T_{sky}}\right) \qquad (10)$$

using the climatological average values of T_{mr} for each month. The residual uncertainty in the regressions, i.e. the variation in the data that is not explained by the regression, is referred to as the theoretical accuracy. That is, even if the observed optical depths were exactly correct some uncertainty in the retrieved values of PWV and LWP would result from the residual uncertainty in the regressions.

3.2 Tuning Functions

Because the model used to compute optical depths and brightness temperatures does not capture all of the physics, "tuning functions" must be developed to linearly relate the actual brightness temperatures observed with the MWR, T_{sky}, to those computed with the model, T_{model} (Westwater *et al.*, 1990). Because

MWRs operated by NOAA/WPL used 20.6 GHz and 31.65 GHz (Hogg *et al.*, 1983) rather than 23.8 and 31.4 GHz, these tuning functions had to be developed after the deployment of the first MWR at the CART site in Oklahoma. This was accomplished by implementing the NOAA/WPL microwave radiation transfer model into the CART data system as a Quality Measurement Experiment or QME. (See Miller *et al.* in this volume.) After the data from each CART Balloon-Borne Sounding System (BBSS) launch was received by the CART data system, the WPL model was run automatically in order to generate model-calculated brightness temperatures and compute the PWV from the sounding for comparison with the MWR. As the number of samples in this database has accumulated, the tuning functions have been periodically revised.

A final adjustment of the tuning functions was necessary in order to eliminate a bias in LWP that caused the MWR to indicate the presence of liquid water for clear sky conditions. This was accomplished using a variation of a procedure developed by L.S. Fedor of NOAA/WPL for the purpose of adjusting the calibration of MWRs operated by NOAA/WPL without tipping curves. In this variation the brightness temperatures required to produce the observed values of PWV with LWP set to zero were computed and a regression against the observed brightness temperatures performed. The results of this procedure are given in Table 2.

Table 2. Slopes and intercepts for tuning functions, $T_{model} = m\ T_{sky} + b$.

	Vapor Channel		Liquid Channel	
	slope	intercept	slope	intercept
QME	0.895	2.27	0.969	-0.549
Adjusted	0.904	0.348	0.968	-0.176
WPL	0.863	0.263	0.982	-0.791

4. PERFORMANCE

4.1 Accuracy of PWV

The results of the QME comparing the PWV from the MWR with that computed from the BBSS for the time period of Figure 1 are presented as a scatter plot in Figure 4. The general impression from this plot is that the agreement for clear sky conditions is superior to cloudy sky conditions. This impression is borne out by comparing the distributions of differences ($PWV_{MWR} - PWV_{BBSS}$) presented in Figure 5. For clear sky conditions the mean difference (i.e. the bias) is essentially zero whereas there is a significant negative bias for cloudy skies. Also, the standard deviation of the clear sky differences is half of that for cloudy skies; the clear sky value equals the theoretical accuracy of the PWV retrieval, so this is as good as the agreement is likely to be.

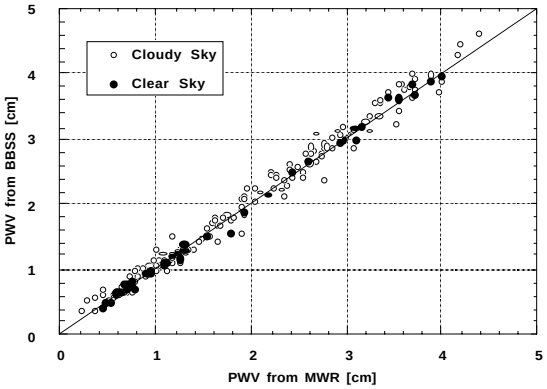

Figure 4. Scatter plot of PWV measured with the MWR against PWV derived from BBSS soundings for clear and cloudy sky conditions though June 1993.

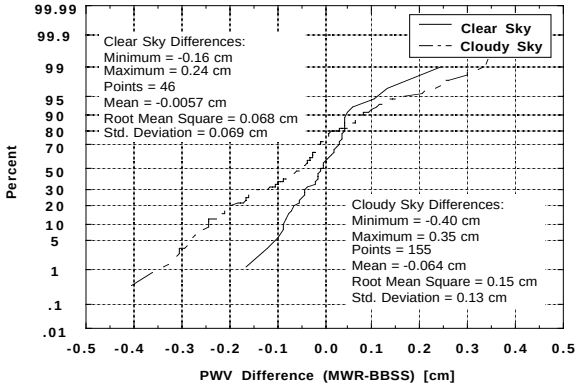

Figure 5. The distribution of differences in PWV between the MWR and BBSS using the data from Figure 4.

The performance of the MWR in terms of PWV accuracy under relatively extreme conditions of high PWV and LWP is presented in Figure 6. The accompanying LWP data are presented in Figure 7. The mean and Root-Mean-Square (RMS) differences between MWR- and BBSS-derived PWV agree with the annual statistics for cloudy skies presented above.

In order to try to understand the relationship between PWV accuracy and cloud cover, the cumulative distribution of RMS differences in PWV as a function of LWP is presented in Figure 8. The cumulative number of BBSS soundings is also plotted; about 25% of the soundings are for clear sky conditions, another 50% occur for LWP less than 0.1 mm; only 25% span the range from 0.1 to 1.5 mm.

Figure 8 reveals a steady increase in the RMS difference with increasing LWP until a value of LWP ≈ 0.3 mm. Several possibilities exist for this increase. First, the horizontal distribution of water vapor may become more inhomogeneous with increasing cloudiness. Because the MWR and BBSS do not sample the same volume of the atmosphere, differences between them should increase as horizontal homogeneity breaks

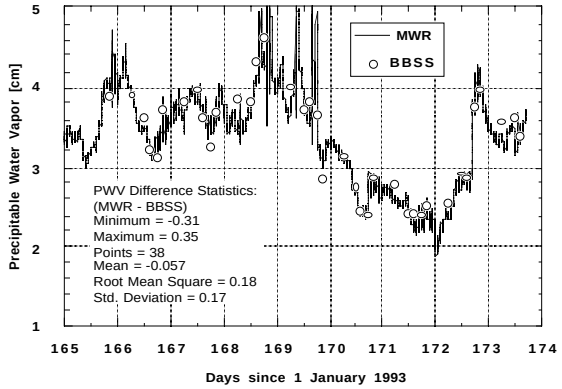

Figure 6. Time series of PWV for 15-23 June 1993.

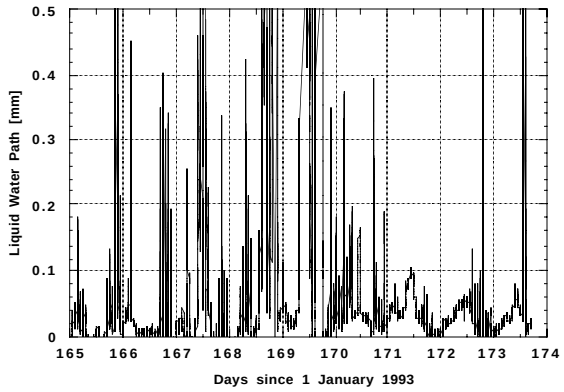

Figure 7. Time series of LWP for 15-23 June 1993.

down. Second, Schmidlin (1988) has shown that radiosondes can exhibit anomalous behavior upon passing from a cloud into clear air. Third, the number of soundings for which the LWP exceeds 0.2 mm is quite limited. If this trend holds generally, then large LWP events represent extremes in the climatology upon which the retrievals are based; i.e., the farther from the statistical average conditions, the greater the error in the retrieval (see Hogg *et al.*, 1983). The latter may be most apparent in the mean radiating temperature, T_{mr}.

The values of T_{mr} used in the present retrieval method represent climatological averages for each month derived from the same historical data as the retrieval coefficients. In Figure 9 these climatological averages are compared against the values computed for each CART BBSS sounding as part of the QME. In general the BBSS-derived values follow the climatological trend well, with the largest discrepancies occurring during the winter months. This may be due, at least in part, to the known difficulties of the NWS sondes (upon which the climatological values are based) at low humidities; see Nash and Schmidlin (1987). However, T_{mr} is strongly affected by the amount of liquid water present. To illustrate this, the values of T_{mr} computed from BBSS soundings for the same period as Figures 6 and 7 are plotted in Figure 10. The climatological averages for June are also plotted for reference. The variation in T_{mr} during this period is approximately half of the annual variation exhibited by the climatological

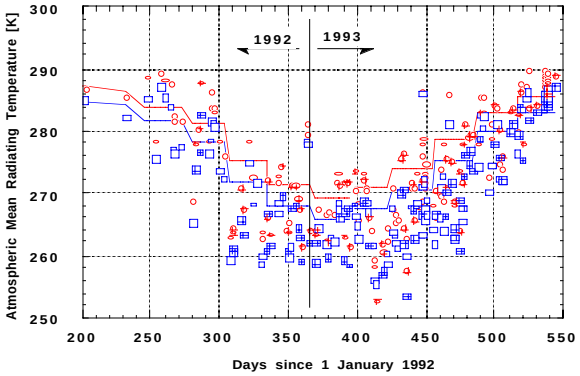

Figure 9. Mean radiating temperatures computed from soundings for 23.8 GHz (circles) and 31.4 GHz (squares) under cloudy sky (open symbols) and clear sky (symbols with '+'s) conditions. The monthly mean values used in the retrievals are indicated as solid lines. ($T_{mr,\ 23.8} > T_{mr,\ 31.4}$)

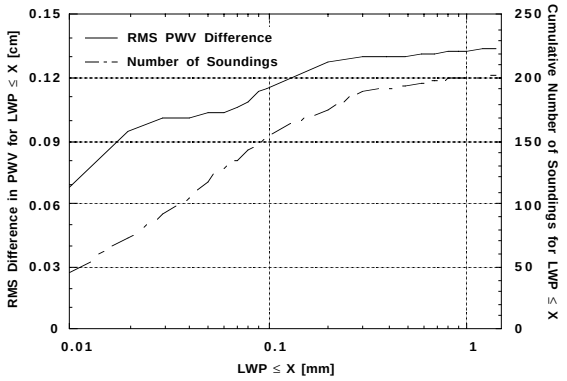

Figure 8. Cumulative distribution of RMS differences in PWV between MWR and BBSS for increasing LWP. The cumulative distribution of soundings according to LWP is also indicated.

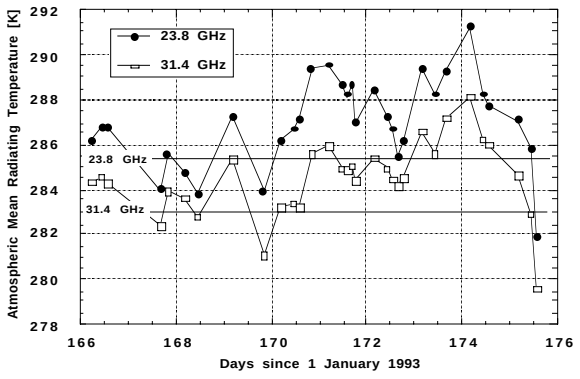

Figure 10. T_{mr} computed from soundings for 16-26 June 1993. Climatological average values for June are indicated as solid lines.

values. Fortunately, the retrieved value of PWV is relatively insensitive to variations in T_{mr} of the order of ± 5 K; unfortunately, the LWP is much more sensitive to T_{mr}.

4.2 Accuracy of LWP

Because the BBSS does not measure liquid water content in clouds, a direct comparison against the MWR-derived values as presented above for PWV is not possible. However, indirect evaluations are possible. For example, Daum (1993) used a parameterization developed by Derr *et al.* (1990) to relate cloud transmittance to LWP and found that the predicted and observed transmittances could not be reconciled without adjusting the observed LWP for a positive bias ranging from 0.01 to 0.05 mm. This was most apparent on cloud-free days because LWP was greater than zero, indicating the presence of clouds. As discussed above, this bias was corrected by adjusting the tuning functions. It should be noted however that the theoretical accuracy of the LWP retrieval is 0.035 mm. This means that there will be some uncertainty under conditions of low LWP as to whether thin clouds are present. (See "Future Improvements" below.)

Daum also pointed out that even after correcting for the bias, the LWP oscillated about zero (± 0.01 mm). This is believed to be due to short term variations in the mean radiating temperature that cannot not be accounted for with the climotological average monthly values. Implementing Derr's parameterization as a QME may enable this situation to be monitored.

4.3 Sensitivity

The application of LWP observations to develop and test models of inhomogeneous cloud structure demand a high sampling rate with a short averaging period. Conflicting with this requirement is the need to achieve a sufficient signal-to-noise ratio to distinguish cloud structure. One way to achieve a high signal-to-noise ratio is to average. However this also smears out the cloud structure. The only solution is to use an instrument with sufficiently low noise characteristics (i.e. high sensitivity) to support a high sampling rate.

Additionally, typical analyses of LWP and PWV time series include measures of *changes* in the data such as spectrum analysis; see Hogg, *et al.*, 1983 or Cahalan and Snider, 1989 for examples. These require high-sensitivity observations of the phenomena.

To determine the sensitivity of the MWR, cloud-free periods were selected from two days: 22 October 1992 during which the PWV varied from 2.5 to 3.0 cm, and 13 January 1993 having a variation in PWV from 0.5 to 1.0 cm. The PWV, LWP and brightness temperatures from these periods (1-second integrations at 20-second intervals) were high-pass filtered using a recursive digital filter having a 2-minute time constant. The 2-minute time constant was determined empirically as that which produced uncorrelated samples. That is, the autocorrelation of the output of the high-pass filter equaled zero after one lag.

This process removed the atmospheric contributions to the signal, leaving behind only the instrument noise. (This is why clear-sky conditions were selected for study; clouds contribute to the signal at much higher frequencies.) The RMS of the high-passed signal is thus the 1-second sensitivity of the instrument*. These values are summarized in Table 3.

Table 3. Summary of MWR Performance

Precipitable Water Vapor (PWV)	
Theoretical Accuracy	0.07 cm
Measured Accuracy (RMS Difference from BBSS)	
Clear sky	0.07 cm
Cloudy sky	0.15 cm
Sensitivity (1-s RMS noise)	0.01 cm
Liquid Water Path (LWP)	
Theoretical Accuracy	0.03 mm
Sensitivity (1-s RMS noise)	0.003 mm
Brightness Temperature	
23.8 GHz Sensitivity (1-s RMS)	0.11 K
31.4 GHz Sensitivity (1-s RMS)	0.14 K
Calibration Stability	
Annual Average	1×10^{-3} month^{-1}

As the values indicate, the sensitivity is an order of magnitude better than the accuracy.

5. FUTURE IMPROVEMENTS

The most vexing problem with the MWR has been associated with the accumulation of water on the Teflon window covering the mirror. Dew, rain, or melting snow on the Teflon window cause the MWR signal to saturate, effectively "drowning" the atmospheric signal. To try to prevent the accumulation of water and to promote evaporation of water that does accumulate, the MWR has a blower that directs a stream of air over the Teflon window. Unfortunately, in condensing environments (e.g. when the temperature falls to the dew point at night or after a heavy rainfall) the air stream is fully saturated and the blower does little good until the relative humidity falls.

---

* Contributions to the 1-second sensitivity due to aliasing of the instrument noise spectrum at frequencies less than about 1 Hz (the integration period) but greater than 0.025 Hz (the Nyquist frequency for 20-second sampling) have not been removed; this would decrease the calulated RMS values.

In order to positively identify such situations a solid-state moisture sensor is being retrofitted to the MWRs. Mounted horizontally, downstream of the Teflon window from the blower, it should get wet when the Teflon window does; because it is farther from the blower, it should not dry until the window dries.

In order to overcome such situations a heater could be mounted in the blower housing and activated by the moisture sensor. However, this would likely increase the maximum power consumption of the instrument by an order of magnitude, from 120 W to 3-4 kW.

In order to identify sky conditions (i.e. clear or cloudy) more accurately during conditions of low LWP, a zenith-viewing infrared thermometer with a spectral response in the 10-11 μm region and a narrow field of view has been acquired for installation on the MWR.

6. CONCLUSIONS

The performance of the WVR-1100 microwave radiometer deployed by ARM at the Oklahoma CART site central facility to provide time series measurements precipitable water vapor (PWV) and liquid water path (LWP) has been presented. The instrument has proven to be durable and reliable in continuous field operation since June, 1992.

The accuracy of the PWV has been demonstrated to achieve the limiting accuracy of the statistical retrieval under clear sky conditions, degrading with increasing LWP. A bias in the LWP has been corrected; uncertainties in the LWP during clear sky conditions are less than the theoretical accuracy of the retrieval. The sensitivity of the PWV and LWP measurements for a 1-second integration is approximately an order of magnitude better than the accuracy.

Improvements are planned to address moisture accumulation on the Teflon window, as well as to identify the presence of clouds with LWP at or below the retrieval uncertainty.

7. ACKNOWLEDGMENTS

The author would like to acknowledge many profitable discussions with E.R. Westwater with respect to this work. Discussions with W.J. Wiscombe and F.S. Solheim were also very helpful. Implementation of the QME by N.E. Miller was essential. This work was supported by the U.S. Department of Energy under Contract DE-AC06-76RLO 1830.

REFERENCES

Cahalan, R.F. and J.B. Snider, 1989: Marine stratocumulus structure. *Remote Sens. Environ.*, **28**, 95-107.

Cahalan, R.F. and W.J. Wiscombe, 1991: Plane Parallel Albedo Bias. *Proceedings of the Second Atmospheric Radiation Measurement (ARM) Science Team Meeting*. Denver, CO. USDOE CONF-9110336.

Daum, P., 1993: SGP/MWR Bias in LWP measurements. ARM Problem Identification Form PIF930610.2.

Derr, V.E., R.S. Stone, L.S. Fedor and H.P. Hanson, 1990: A parameterization for the shortwave transmissivity of stratiform water clouds based on empirical data and radiative transfer theory. *J. Atmos. Sci.*, **47**, 2774-2783.

Decker, M.T. and J.A. Schroeder, 1991: Calibration of ground-based microwave radiometers for atmospheric remote sensing. NOAA Tech Memo ERL WPL-197.

Hogg, D. C., F. O. Guiraud, J. B. Snider, M. T. Decker and E. R. Westwater, 1983: A steerable dual-channel microwave radiometer for measurement of water vapor and liquid in the troposphere. *J. Clim. Appl. Meteorol.*, **22**, 789-806.

Kuo, Y-H., Y-R. Guo and E.R. Westwater, 1993: Assimilation of precipitable water measurements into a mesoscale numerical model. *Mon. Wea. Rev.*, **121**, 1215-1238.

Li, Z., H.G. Leighton and R.D. Cess, 1992: Surface net solar radiation estimated from satellite measurements: comparisons with tower observations. Submitted to *J. Climate*.

Miller, N.E., J.C. Liljegren, T.R. Shippert, S.A. Clough, and P.D. Brown 1994: Quality Measurement Experiments within the Atmospheric Radiation Measurement Program. *74th AMS Annual Meeting*. Nashville, TN.

Nash, J. and F.J. Schmidlin, 1987: WMO international radiosonde comparison, phase I. *Instruments and Observing Methods Report No. 30* WMO/TD-195.

Schmidlin, F.J., 1988: WMO international radiosonde comparison, phase II. *Instruments and Observing Methods Report No. 29*. WMO/TD-312.

Schroeder, J.A. and E.R. Westwater, 1991: User's guide to WPL microwave transfer software. NOAA Tech Memo ERL WPL-213.

Stephens, G.L., 1978: Radiative properties of extended water clouds. Parts I and II. *J. Atmos. Sci.*, **35**, 2111-2132.

Stephens, G.L., 1984: The parameterization of radiation for numerical weather prediction and climate models. *Mon. Wea. Rev.*, **112**, 826-867.

Westwater, E.R., 1993: Ground-based microwave remote sensing of meteorological variables. *Remote Sensing by Microwave Radiometry*, M.A. Janssen, ed. John Wiley & Sons.

Fifth Symposium on Global Change Studies, January 23-28, 1994, Nashville, TN, pp. 262-269. American Meteorological Society.

Westwater, E. R., J. B. Snider and M. J. Falls, 1990: Ground-based radiometric observations of atmospheric emission and attenuation at 20.6, 31.65 and 90.0 GHz: a comparison of measurements and theory. *IEEE Trans. Antenn. and Propag.*, **38**, 1569-1580.

U.S. Department of Energy, 1990: Atmospheric Radiation Measurement Program Plan. DOE/ER-0441.